

Real Space Picture of Collective Excitation in Sr₂CuO₃

C. Eichstaedt,^{1,2} A. Eguluz,^{1,2} A. Kozhevnikov,³

¹Department of Physics and Astronomy, University of Tennessee Knoxville, Knoxville, 37996, USA

²Joint Institute for Advanced Materials, University of Tennessee Knoxville, Knoxville, 37996, USA

³Swiss National Supercomputer Center, ETH Zurich, CH-8093 Manno, Switzerland

I. Experimental Motivation

In early work the term ‘plasmon’ was coined by David Pines to describe the *collective excitations* of materials that exhibit free electron like behavior, i.e. simple metals. The plasmon was originally defined as a zero (or local minimum) in the real part of the longitudinal dielectric function $\varepsilon(\vec{q} \rightarrow 0, \omega_p)$; and is visualized as the entire electron gas oscillating with frequency ω_p . The ideal probe measuring ‘plasmons’ is a beam of *fast* electrons, which couple directly to the electron density of the sample, using the the probing technique Electron Energy Loss Spectroscopy (EELS). EELS has a cross section that measures $Im[-1/\varepsilon(\vec{q}, \omega)]$, so the strongest signals in small momentum transfer regime correspond to ‘plasmons’.

One would not expect that this collective phenomenon to appear in materials where the relevant degrees of freedom are though to be localized. Contrary to this viewpoint, in EELS measurements, Sr₂CuO₃ shows a collective excitation that disperses from 2.6-3.2 eV for wave vector \vec{q} in the first Brillouin Zone shown in fig. 1b). In addition, using the first principles formalism of Time-Dependent Density Functional Theory (TD-DFT), using the Random-Phase Approximation (RPA), calculated from a DFT^{1,2}+U ground state (U=4 eV J=1 eV), the dispersion is within well-agreement with the experiment⁴, shown in fig 1b) using all bands in fig 1c).

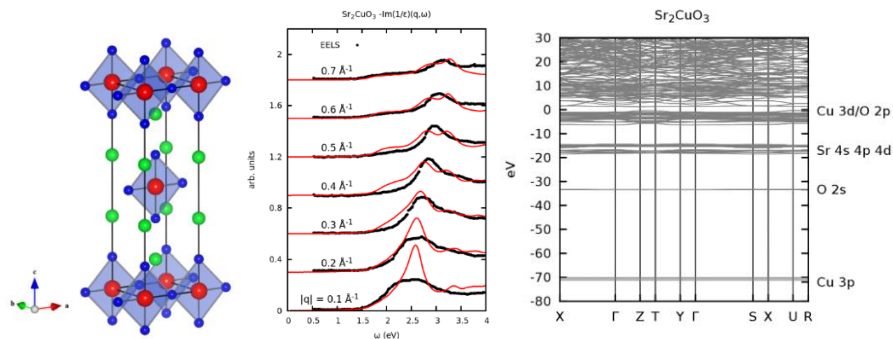


FIG. 1. a) Conventional unit cell for Sr₂CuO₃. b) Dispersion for the measured (black) and calculated (red) loss function. c) Band structure used in the calculation of the density response function calculated using TD-DFT.

II. Downfolded Hilbert Space

To understand this excitation and ‘open up’ the black box behind the red curves in fig 1b), a local basis of spin-resolved Wannier orbitals $W_{n\sigma}(\vec{x} - \vec{R})$ is constructed from the Bloch states $\psi_{\vec{k}j\sigma}(\vec{x})$ using the unitary transformation

$$W_{n\sigma}(\vec{x} - \vec{R}) = \frac{1}{\sqrt{N_{BvK}}} \sum_{\vec{k}} e^{-i\vec{k}\cdot\vec{R}} \sum_{j=n_1(\vec{k})}^{n_2(\vec{k})} a_{nj\sigma}(\vec{k}) \psi_{\vec{k}j\sigma}(\vec{x})$$

To agree with experiment, the minimum Hilbert space needed is 1 occupied and 1 unoccupied $x^2 - y^2$ orbital per spin and chain¹ shown in fig 2.

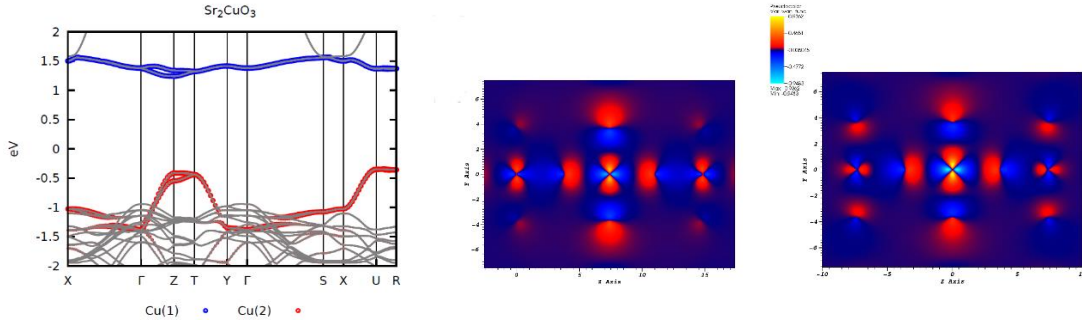


FIG. 2. a) Shows the orbital weight of the Wannier functions as a function of the underlying Bloch states. b) and c) show the Wannier projection for an occupied and unoccupied orbital respectively. For relevance, the occupied orbital red in a) encompasses the chemistry of the Zhang-Rice singlet and the unoccupied orbital entails physics of the ‘upper-Hubbard band’.

III. Downfolding Response

The loss function is related to the retarded density-density response $\chi(\vec{q}, \omega)$ and the Fourier transform of the bare Coloumb interaction $v(\vec{q})$ function using $1/\epsilon(\vec{q}, \omega) = 1 + v(\vec{q})\chi(\vec{q}, \omega)$

Within TD-DFT, χ can be calculated through the matrix equation

¹ The 2 relevant chains in the antiferromagnetic a unit cell can be visualized in fig 1a) as the top chain of Cu-O plaquettes (the ones shifted to the right) and the middle chain of plaquettes where only of the plaquettes of the chain is visible.

$$\chi_{\vec{G}\vec{G}'}(\vec{q}, \omega) = (\chi_s)_{\vec{G}\vec{G}'}(\vec{q}, \omega) + \sum_{\vec{G}_1\vec{G}_2} (\chi_s)_{\vec{G}\vec{G}_1}(\vec{q}, \omega) \left[v(\vec{q} + \vec{G}_1) \delta_{\vec{G}_1\vec{G}_2} + f_{\vec{G}_1\vec{G}_2}^{xc}(\vec{q}, \omega) \right] \chi_{\vec{G}_2\vec{G}'}(\vec{q}, \omega) \quad (1)$$

Where the non-interacting polarizability χ_s is given through the bare 2 -particle propagator⁵, using the basis we defined in section II ,

$$(\chi_s)_{\vec{G}\vec{G}'}(\vec{q}, \omega) = \sum_{\vec{R}\vec{R}'} \sum_{n_1 n_2} \sum_{\sigma} A_{\vec{0}n_1\sigma; \vec{R}n_2\sigma}(\vec{q} + \vec{G}) (\tilde{\chi}_s)_{\vec{0}n_1\sigma; \vec{R}n_2\sigma}^{\vec{0}n_1'\sigma; \vec{R}n_2'\sigma}(\vec{q}, \omega) A_{\vec{0}n_1'\sigma; \vec{R}n_3\sigma}^*(\vec{q} + \vec{G}') \quad (2)$$

By working in the RPA, i.e by setting $f^{xc} = 0$ in equation 1, the density response function is calculated through the dressed 2-particle propagator⁵ $\tilde{\chi}$

$$\chi_{\vec{G}\vec{G}'}(\vec{q}, \omega) = \sum_{\vec{R}\vec{R}'} \sum_{n_1 n_2} \sum_{\sigma\sigma'} A_{\vec{0}n_1\sigma; \vec{R}n_2\sigma}(\vec{q} + \vec{G}) (\tilde{\chi})_{\vec{0}n_1\sigma; \vec{R}n_2\sigma}^{\vec{0}n_1'\sigma'; \vec{R}n_2'\sigma'}(\vec{q}, \omega) A_{\vec{0}n_1'\sigma'; \vec{R}n_3\sigma'}^*(\vec{q} + \vec{G}') \quad (3)$$

Where the A terms are the amplitudes for charge fluctuations in the Wannier basis and $\tilde{\chi}$ satisfies the Bethe-Salpeter equation (noting that $\tilde{\chi}_s$ is diagonal in the spin index shown in equation 2)

$$\begin{aligned} & (\tilde{\chi})_{\vec{0}n_1\sigma; \vec{R}n_2\sigma}^{\vec{0}n_1'\sigma'; \vec{R}n_2'\sigma'}(\vec{q}, \omega) \\ &= (\tilde{\chi}_s)_{\vec{0}n_1\sigma; \vec{R}n_2\sigma}^{\vec{0}n_1'\sigma'; \vec{R}n_2'\sigma'}(\vec{q}, \omega) \\ &+ \sum_{\vec{R}_1\vec{R}_1'} \sum_{n_1 n_2} \sum_{\sigma_1\sigma_1'} (\tilde{\chi}_s)_{\vec{0}n_1\sigma; \vec{R}_1n_2\sigma}^{\vec{0}n_3\sigma_1; \vec{R}_1n_4\sigma_1}(\vec{q}, \omega) \tilde{V}_{\vec{0}n_3\sigma_1; \vec{R}_1n_4\sigma_1}^{\vec{0}n_3'\sigma_1'; \vec{R}_1n_4'\sigma_1'}(\vec{q}, \omega) (\tilde{\chi})_{\vec{0}n_3'\sigma_1'; \vec{R}_1n_4'\sigma_1'}^{\vec{0}n_1'\sigma'; \vec{R}n_2'\sigma'}(\vec{q}, \omega) \end{aligned}$$

Due to the localization of the orbitals seen in fig b,c), the summation over lattice vectors \vec{R} can be truncated to NP-CF with good agreement to equations 2 and 3.² Experimentally, these quantities give theoretical calculations for optical conductivity³ and EELS loss function. It is

² The results agree extremely well with the ‘blackbox’ calculations when including 3NP-CF.

³ The value for the Hubbard U (4 eV) in the DFT+U ground state calculation was chosen to fit the optical peak. It is worth noting that the experimental measurement and the theoretical calculation are both calculated in absolute units.

shown in fig 3a) that the single-particle excitation spectrum is primarily saturated with 1D NP-CF along the chain consistent with current one-dimensional fermiology description of Sr₂CuO₃.

However, when it comes to solving the 2-particle problem (even at the level of RPA) both chains in the antiferromagnetic unit cell have to be included to capture the ‘plasmon’ dispersion, seen in fig. 3b as the difference between the grey and the red curve. To understand the emergence of the pole using a local basis which symbolically is $\tilde{\chi} = \tilde{\chi}_s(1 - \tilde{V}\tilde{\chi}_s)^{-1}$, and since Wannier orbitals are not eigenstates of the Hamiltonian (even at the non-interacting level), to see the emergence of a pole, the relevant quantity is $\det(1 - \tilde{V}\tilde{\chi}_s)$ shown in fig 3c).

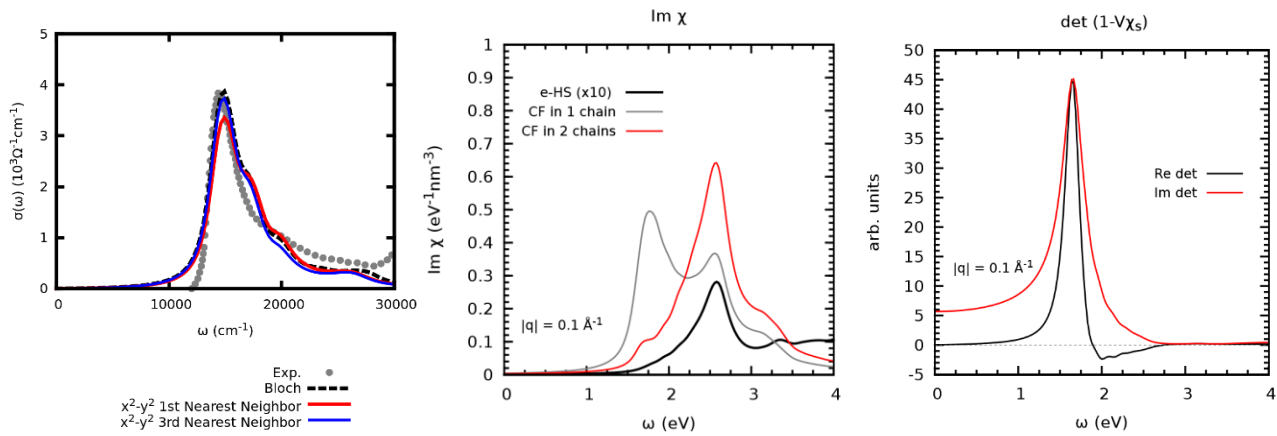


FIG. 3. a) Optical conductivity measurement³ and calculation using absolute units. b) χ calculated using 1 chain (gray), 2-chain (red), and the ‘blackbox’ calculation. It should be noted that the differences in intensities can be corrected for by renormalizing the A-amplitudes given in equation 2 and 3. c) The equivalent of the dielectric function derived from a local basis.

There are 2 main takeaway messages here. The first being that the relevant degrees of freedom are not the same for all experimental probe. This can be seen in that the optical conductivity can be reproduced with electrons in 1-chain of Sr₂CuO₃, while the loss function in EELS experiments require that 2 chains be included in the calculation due to the long range nature for the electron-electron interaction (bare and screened). The second message here is that the collective excitation in Sr₂CuO₃ can be understood using a few orbitals in a local basis contrary to conventional plasmons that need the entire crystal to collectively cooperate.

REFERENCES

- ¹P. Hohenberg and W. Kohn, Phys. Rev. **136**, B864 (1964).
- ²W. Kohn and L. J. Sham, Phys. Rev. **140**, A1133 (1965).
- ³K.W Kim and G.D Gu, Phys. Rev. B. **79**, 085121 (2009).
- ⁴J. Fink et. al, Journal of Electron Spectroscopy. **117-118**, 287-309 (2001).
- ⁵W. Hanke and L. J. Sham, Phys. Rev. B. **12**, 4501 (1975).